Journal of Solid State Chemistry **147,** 350–357 (1999)
Article ID jssc.1999.8337, available online at http://www.idealibrary.com on IDEAL®

Tantalum Chlorides in Octahedral Cluster Chemistry: The Structures of $Cs_2PbTa_6Cl_{18}$ and $CsPbTa_6Cl_{18}$

S. Cordier, C. Loisel, C. Perrin,[1] and M. Sergent

Laboratoire de Chimie du Solide et Inorganique Moléculaire, UMR 6511, Université de Rennes 1, Campus de Beaulieu, Avenue du Général Leclerc, 35042 Rennes Cedex, France

Received December 15, 1998; in revised form March 30, 1999; accepted April 21, 1999

Two new series of Ta_6 chlorides, $Cs_2M'^{II}Ta_6Cl_{18}$ and $CsM'^{II}Ta_6Cl_{18}$, have been isolated with $M' = Ba^{2+}$, Pb^{2+}, Sr^{2+}, Eu^{2+}, Ca^{2+}. From single-crystal structure refinements the compounds $Cs_2PbTa_6Cl_{18}$ [*R*-3, $Z = 1$, $a = 10.291(2)$ Å, $\alpha = 54.645(8)^\circ$] and $CsPbTa_6Cl_{18}$ [*P*-31*c*, $Z = 2$, $a = 9.2673(8)$ Å, $c = 17.249(3)$ Å] are isotypic with $KLuNb_6Cl_{18}$ and $CsLuNb_6Cl_{18}$, respectively. In the former compound the structure consists of a fcc stacking of Ta_6Cl_{18} units, while a pseudohexagonal $AA'A$ stacking of units is observed for the latter compound. The tetrahedral site of units, half-occupied by K^+ in $KLuNb_6Cl_{18}$ is fully occupied by Cs^+ in $Cs_2PbTa_6Cl_{18}$. The interatomic distances are consistent with valence electron concentrations per cluster (VEC) of 16 and 15 for $Cs_2PbTa_6Cl_{18}$ and $CsPbTa_6Cl_{18}$, respectively. It is the first time that such a VEC of 15 is observed for a quaternary Me_6X_{18}-unit based compound; this feature is discussed in relation to the density functional theory results previously reported on Me_6X_{18} (Me = Nb, Ta; X = Cl, Br). © 1999 Academic Press

***Key Words*: Ta_6 clusters; chlorides; synthesis; crystal structure.**

I. INTRODUCTION

These last years, in niobium and tantalum edge-bridged octahedral cluster chemistry, we have investigated new materials with the formula $M_xREMe_6X_{18}$ (M = monovalent cation; $x = 0$, 1, or 2; RE = rare earth cation; Me = Nb or Ta; and X = Cl or Br) exhibiting a valence electron concentration (VEC) per Me_6 cluster of 16 or 15 (1). These compounds, based on discrete Me_6X_{18} units, crystallize in two structure types, $KLuNb_6Cl_{18}$ (trigonal, *R*-3) (2) and $CsLuNb_6Cl_{18}$ (trigonal, *P*-31*c*) (3), depending on electronic or steric effects related to the cationic charges and to the sizes of the cations and ligands, respectively. In the *R*-3 structure type the site of the monovalent cation is filled in $M_2RE^{II}Me_6X_{18}$ (VEC = 16), half-filled in $MRE^{III}Me_6X_{18}$ (VEC = 16), and empty in $RE^{III}Me_6X_{18}$ (VEC = 15), while it is always filled in the *P*-31*c* structure type.

Recently, in $K_2MnNb_6Cl_{18}$ (4) with the *R*-3 structure type, the rare earth has been replaced by the Mn^{2+} divalent cation, leading to a VEC of 16. Up to now, such a replacement has never been performed for the *P*-31*c* structure type which has always been obtained with a trivalent rare earth.

In this paper we present two new Ta_6 cluster series with a divalent cation in place of the rare earth cation: $Cs_2M'^{II}Ta_6Cl_{18}$ (*R*-3, VEC = 16) and $CsM'^{II}Ta_6Cl_{18}$ (*P*-31*c*, VEC = 15). It is the first time that a quaternary Ta_6 compound with a VEC of 15 has been isolated. These original Ta_6 chlorides constitute new experimental results for the investigation of the electronic structure of $(Me_6X_{18})^{n-}$- based compounds and give additional support to our recent theoretical study (5).

II. EXPERIMENTAL

1. Synthesis of the $Cs_2M'^{II}Ta_6Cl_{18}$ and $CsM'^{II}Ta_6Cl_{18}$ Chlorides

The $Cs_2M'^{II}Ta_6Cl_{18}$ and $CsM'^{II}Ta_6Cl_{18}$ chlorides have been isolated for $M'^{2+} = Ba^{2+}$, Pb^{2+}, Sr^{2+}, Eu^{2+}, and Ca^{2+}. The compounds of the two series were synthesized by solid-state reactions from stoichiometric mixtures of $TaCl_5$ (Alfa 99.9%), Ta (Alfa m3N, t2N6), $M'Cl_2$, and CsCl (Prolabo, 99.5%). The mixtures handled under dry atmosphere are pelletized and heated with some pieces of tantalum foil at temperatures ranging from 600 to 700°C for 24 h in a sealed silica tube. All compounds are obtained in the form of a microcrystalline powder. They are stable in air and are green and brown for $Cs_2M'^{II}Ta_6Cl_{18}$ and $CsM'^{II}Ta_6Cl_{18}$ respectively. We note that it is very difficult to obtain these new quaternary chlorides with a good degree of purity. Indeed, some additional diffraction peaks of small intensity, attributed to Ta_6Cl_{15} (6), are always observed in the X-ray powder patterns. The latter secondary phase is also identified by microprobe analysis.

[1] To whom correspondence should be addressed. E-mail: christiane.perrin@univ-rennes1.fr. Fax: (33) 2.99.63.57.04.

0022-4596/99 $30.00

X-ray studies indicate that $Cs_2M'^{II}Ta_6Cl_{18}$ and $CsM'^{II}Ta_6Cl_{18}$ are isotypical with $KLuNb_6Cl_{18}$ (*R*-3) and $CsLuNb_6Cl_{18}$ (*P*-31*c*), respectively. The unit-cell constants were first determined from X-ray diffraction powder patterns with silicium as internal standard, recorded on a INEL CPS 120 diffractometer using Cu$K\alpha_1$ radiation. They were refined by least-square calculations and are given in Tables 1 and 2. For these two series the evolution of the unit-cell volume versus the ionic radius of the divalent cation is represented in Fig. 1. A good correlation is observed, indicating that europium is in the divalent state in the two corresponding compounds. It must be recalled that our previous works had shown that europium was always trivalent in the other *P*-31*c* series, while it could be divalent or trivalent in the *R*-3 one but with two different stoichiometries: $M_2Eu^{II}Me_6X_{18}$ and $MEu^{III}Me_6X_{18}$ (1).

Single crystals of all these compounds are difficult to obtain. In a general way, we have observed that it is more difficult to obtain single crystals in the Ta_6 chemistry than in the Nb_6 chemistry. However, we have succeeded in growing single crystals of $Cs_2PbTa_6Cl_{18}$ and $CsPbTa_6Cl_{18}$ suitable for structural determination during syntheses of 1 month at 650°C.

2. *Crystal Data and Structural Determinations of $Cs_2PbTa_6Cl_{18}$ and $CsPbTa_6Cl_{18}$*

For $Cs_2PbTa_6Cl_{18}$ and $CsPbTa_6Cl_{18}$ the intensity data were recorded with a Nonius CAD4 diffractometer, at room temperature. The experimental conditions for data collection are given in Tables 3 and 4. The unit-cell constants of the two compounds were refined on single crystals from 25 reflections.

Intensity data treatment and refinement calculations were performed using the MOLEN programs from Enraf Nonius (10) on a Digital Micro VAX 3100. The details are given in Tables 3 and 4. The measured intensities were corrected for Lorentz and polarization effects. Absorption corrections were applied: ΨSCAN from 7 reflections for $CsPbTa_6Cl_{18}$ and an empirical absorption correction for $Cs_2PbTa_6Cl_{18}$.

The structure was solved in the *R*-3 space group for $Cs_2PbTa_6Cl_{18}$ and *P*-31*c* space group for $CsPbTa_6Cl_{18}$, based on the initial models of $KLuNb_6Cl_{18}$ and $CsLuNb_6Cl_{18}$, respectively. All atomic positions were found to be fully occupied.

The atomic positional parameters and isotropic equivalent thermal factors are reported in Tables 5 and 6 and the interatomic distances and angles are given in Tables 7 and 8 for $Cs_2PbTa_6Cl_{18}$ and $CsPbTa_6Cl_{18}$, respectively. Additional materials, anisotropic thermal parameters, and observed and calculated structure factors can be obtained on request from the authors.

TABLE 1
Unit-Cell Constants of the $CsM'Ta_6Cl_{18}$ Compounds

M'	Ba	Pb	Sr	Eu	Ca
a (Å)	9.368(2)	9.269(2)	9.283(3)	9.267(2)	8.994(4)
c (Å)	17.306(7)	17.205(5)	17.227(6)	17.281(4)	17.282(9)
V (Å^3)	1315(1)	1280(1)	1285(1)	1285(1)	1210(1)

TABLE 2
Hexagonal and Rhombohedral Unit-Cell Constants of the $Cs_2M'Ta_6Cl_{18}$ Compounds

M'	Ba	Pb	Sr	Eu	Ca
a (Å)	9.581(2)	9.460(2)	9.476(2)	9.471(2)	9.396(2)
c (Å)	26.481(4)	26.152(4)	26.176(4)	26.164(4)	25.851(5)
V (Å^3)	2105(2)	2027(1)	2035(2)	2032(1)	1976(1)
a (Å)	10.417(7)	10.287(4)	10.298(5)	10.293(5)	10.182(5)
α (°)	54.76(1)	54.74(1)	54.78(1)	54.78(1)	54.95(1)

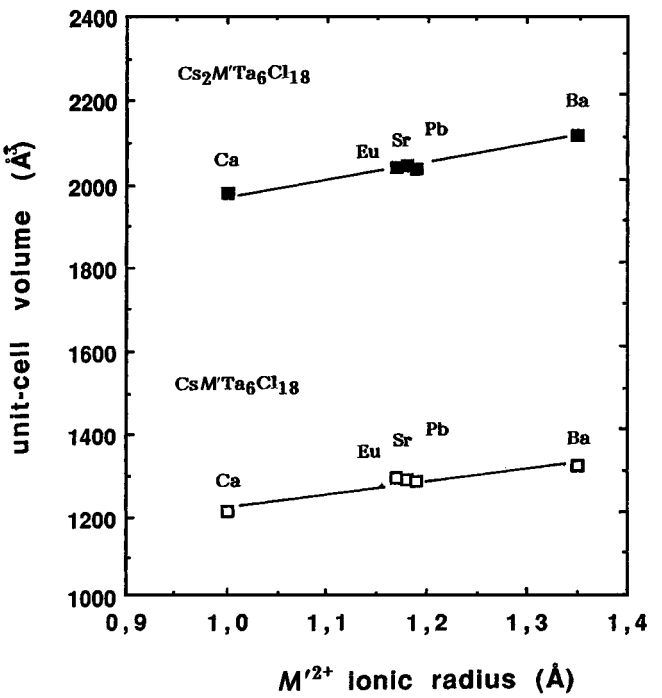

FIG. 1. Evolution of the unit-cell volume versus the ionic radius of the divalent cation for the two series $Cs_2M'Ta_6Cl_{18}$ and $CsM'Ta_6Cl_{18}$. The error bars are smaller than the symbol sizes.

TABLE 3
Crystal Data and Experimental Conditions for Data Collection and Structural Determination of $Cs_2PbTa_6Cl_{18}$[a]

I. Crystal data	
Formula: $Cs_2PbTa_6Cl_{18}$	$M = 2196.8$ g/mol
Crystal system: trigonal	Space group: R-3, No. 148
$a = 10.291(2)$ Å, $\alpha = 54.645(8)^\circ$	$V = 674.6(2)$ Å^3
Unit cell refined from 25 reflection ($4^\circ < \theta < 15^\circ$)	
$\rho_{cal} = 5.41$ g cm^{-3}	$Z = 1$
Crystal size: $0.07 \times 0.07 \times 0.09$ mm^3	
Linear absorption factor: 34.66 mm^{-1}	
II. Data collections	
Temperature: 295 K	Wavelength: Mo$K\alpha$ radiation
Diffractometer: Enraf Nonius CAD-4	Scan mode: ω–2θ
Monochromator: graphite	Scan width: $1.20 + 0.35$ tg θ
$0 < h < 16$; $-16 < k < 16$; $0 < l < 16$	$\theta_{max} = 35^\circ$
3 standard reflections	
2209 measured reflections	
1717 independent reflections	
[with $I > \sigma(I)$]	$R_{int} = 0.015$
III. Structure determination	
Lorentz and polarization corrections	
Absorption correction empirical: [DIFABS (7)]	$T_{min} = 0.94$, $T_{max} = 1.11$
Refinement on F	
1532 independent reflections with $I > 3\sigma(I)$	
Refined parameters: 43	
Unweighted agreement factor $R = 0.026$	
Weighted agreement factor $R_w = 0.042$	$\omega = 4F_0^2/[\sigma^2(F_0^2) + (0.05F_0^2)^2]$
$S = 1.144$	$(\Delta/\sigma)_{max} < 0.02$
$\Delta\rho_{max} = 1.8(4)$ e Å^{-3}	
Extinction correction (8)	Extinction coefficient: $1.5(1) \times 10^{-7}$

[a] Atomic scattering factor from "International Tables for X-ray Crystallography" (9).

TABLE 4
Crystal Data and Experimental Conditions for Data Collection and Structural Determination of $CsPbTa_6Cl_{18}$[a]

I. Crystal data	
Formula: $CsPbTa_6Cl_{18}$	$M = 2063.9$ g/mol
Crystal system: trigonal	Space group: P-31c, No. 163
$a = 9.2673(8)$ Å, $c = 17.249(3)$ Å	$V = 1282.9(3)$ Å^3
Unit cell refined from 25 reflection ($6^\circ < \theta < 16^\circ$)	
$\rho_{cal} = 5.34$ g cm^{-3}	$Z = 2$
Crystal size: $0.09 \times 0.11 \times 0.14$ mm^3	
Linear absorption factor: 35.06 mm^{-1}	
II. Data collections	
Temperature: 295 K	Wavelength: Mo$K\alpha$ radiation
Diffractometer: Enraf Nonius CAD-4	Scan mode: ω–2θ
Monochromator: graphite	Scan width: $1.20 + 0.35$ tg θ
$0 < h < 14$, $0 < k < 14$, $-27 < l < 27$	$\theta_{max} = 35^\circ$
ψScan from 7 reflections	$T_{min} = 0.86$, $T_{max} = 0.99$
3 standard reflections	
2335 measured reflections	
1563 independent reflections	
[with $I > \sigma(I)$]	$R_{int} = 0.020$
III. Structure determination	
Lorentz and polarization corrections	
Refinement on F	
1392 independent reflections with $I > 3\sigma(I)$	
Refined parameters: 42	
Unweighted agreement factor $R = 0.033$	
Weighted agreement factor $R_w = 0.043$	$\omega = 4F_0^2/[\sigma^2(F_0^2) + (0.05F_0^2)^2]$
$S = 1.125$	$(\Delta/\sigma)_{max} < 0.04$
$\Delta\rho_{max} = 2.5(4)$ e Å^{-3}	
Extinction correction (8)	Extinction coefficient: $1.76(5) \times 10^{-7}$

[a] Atomic scattering factor from "International Tables for X-ray Crystallography" (9).

III. RESULTS

1. *Description of the $Cs_2PbTa_6Cl_{18}$ and $CsPbTa_6Cl_{18}$ Structures*

These two structures are based on the $(Ta_6Cl_{18})^{n-}$ units of D_{3d} symmetry, in which the octahedral Ta_6 cluster is edge-capped by 12 inner chlorine atoms (Cl^i) and linked to six additional apical chlorine atoms (Cl^a). This unit is represented in Fig. 2.

In $Cs_2PbTa_6Cl_{18}$ the units are located on the center of the rhombohedral unit cell, giving a fcc stacking. The successive $ABC\ldots$ layers of units are represented in Fig. 3. Pb^{2+} lies at the origin of the rhombohedral unit cell and Cs^+ on the threefold axis. The latter cation fully occupies its sites, in contrast to $KLuNb_6Cl_{18}$ structure for which the K^+ site was only half-occupied. It must be recalled that for the isotypical $Cs_2EuNb_6Br_{18}$ bromide this site was also fully occupied by Cs^+ (11). The two cationic sites are represented in Fig. 4: they consist of a 12Cl environment for Cs^+ and a 6Cl environment for Pb^{2+}, the latter corresponding to a slightly distorted octahedron.

In $CsPbTa_6Cl_{18}$ the units are located on the threefold axes of the trigonal unit cell, forming a pseudohexagonal

TABLE 5
Positional Parameters, Isotropic Equivalent Thermal Factors, and Their Estimated Standard Deviations for $Cs_2PbTa_6Cl_{18}$

Atom	Position	x	y	z	B (Å^2)
Ta	6f	0.29877(3)	0.64656(3)	0.41967(3)	0.611(5)
Cl1	6f	0.9605(2)	0.1714(2)	0.6764(2)	1.43(4)
Cl2	6f	0.1643(2)	0.4341(2)	0.5798(2)	1.06(3)
Cl3	6f	0.7716(2)	0.6426(2)	0.0875(2)	1.15(3)
Pb	1a	0	0	0	0.983(3)
Cs	2c	0.27672(4)	0.277	0.277	1.680(4)

Note. The isotropic equivalent displacement parameter is defined as $\frac{4}{3}[a^2B(1,1) + b^2B(2,2) + c^2B(3,3) + ab(\cos\gamma)B(1,2) + ac(\cos\beta)B(1,3) + bc(\cos\alpha)B(2,3)]$.

TABLE 6
Positional Parameters, Isotropic Equivalent Thermal Factors, and Their Estimated Standard Deviations for $CsPbTa_6Cl_{18}$

Atom	Position	x	y	z	B (Å^2)
Ta	12i	0.83256(3)	0.02686(3)	0.06914(2)	0.488(4)
Cl1	12i	0.6215(2)	0.0542(3)	0.1559(1)	1.37(4)
Cl2	12i	0.4222(2)	0.1642(2)	0.9998(1)	1.08(3)
Cl3	12i	0.0302(2)	0.2265(2)	0.1615(1)	1.04(3)
Pb	2d	2/3	1/3	1/4	1.070(9)
Cs	2c	1/3	2/3	1/4	3.21(4)

Note. The isotropic equivalent displacement parameter is defined as $\frac{4}{3}[a^2B(1,1) + b^2B(2,2) + c^2B(3,3) + ab(\cos\gamma)B(1,2) + ac(\cos\beta)B(1,3) + bc(\cos\alpha)B(2,3)]$.

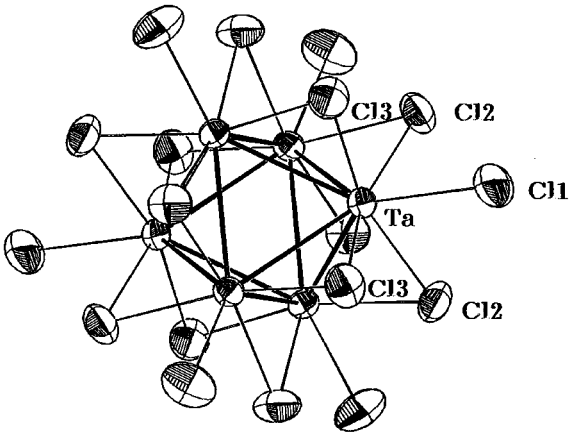

FIG. 2. $(Ta_6Cl^i_{12})Cl^a_6$ unit in the $Cs_2PbTa_6Cl_{18}$ structure.

$AA'A$ stacking, in which the units of the A' layer are rotated by about 20° with respect to the units of the A layer (Fig. 5). The Pb^{2+} and Cs^+ cations are located at 2/3, 1/3, 1/4 and 1/3, 2/3, 1/4 respectively. Their Cl coordination numbers are similar to those in the $Cs_2PbTa_6Cl_{18}$ structure but their coordination polyhedra are different. Indeed, in $CsPbTa_6Cl_{18}$ the Pb^{2+} site is an octahedron of chlorine atoms more distorted than in $Cs_2PbTa_6Cl_{18}$ (Fig. 6). Furthermore, the Cs^+ site is now composed of two 6Cl rings largely opened around the threefold axis above and below Cs^+, giving a possibility of motion along this axis, which leads to a large and anisotropic thermal factor for this cation (Fig. 6). This

TABLE 7
Interatomic Distances (Å) and Angles (°) for $Cs_2PbTa_6Cl_{18}$

	Ta_6 cluster		
Ta–Ta	2.8892(5)	Ta–Ta–Ta	59.974(7)
Ta–Ta	2.8869(5)	Ta–Ta–Ta	60.05(1)
	$(Ta_6Cl_{12})Cl_6$ unit		
Ta–Cl1	2.595(2)	Cl3–Ta–Cl1	81.25(7)
Ta–Cl2	2.471(2)	Cl2–Ta–Cl1	79.85(7)
Ta–Cl2	2.463(2)	Cl2–Ta–Cl1	82.02(7)
Ta–Cl3	2.460(2)	Cl3–Ta–Cl1	80.51(7)
Ta–Cl3	2.456(2)		
Cl2–Cl3	3.416(3)	Cl3–Cl2–Cl2	90.25(7)
Cl2–Cl3	3.455(3)	Cl3–Cl2–Cl2	59.97(2)
Cl2–Cl2	3.450(4)	Cl2–Cl3–Cl3	60.01(6)
Cl3–Cl3	3.434(2)	Cl2–Cl3–Cl3	90.65(7)
	Lead environment		
Pb–Cl1	2.882(2)	Cl1–Pb–Cl1	90.30(6)
	Cesium environment		
Cs–Cl1	3.481(1)		
Cs–Cl3	3.614(1)		
	Shortest other distances		
Pb–Cs	5.652(1)		
Pb–Pb	9.448(1)		
Cs–Cs	6.208(1)		
Ta–Pb	5.058(2)		
Ta–Cs	4.636(2)		

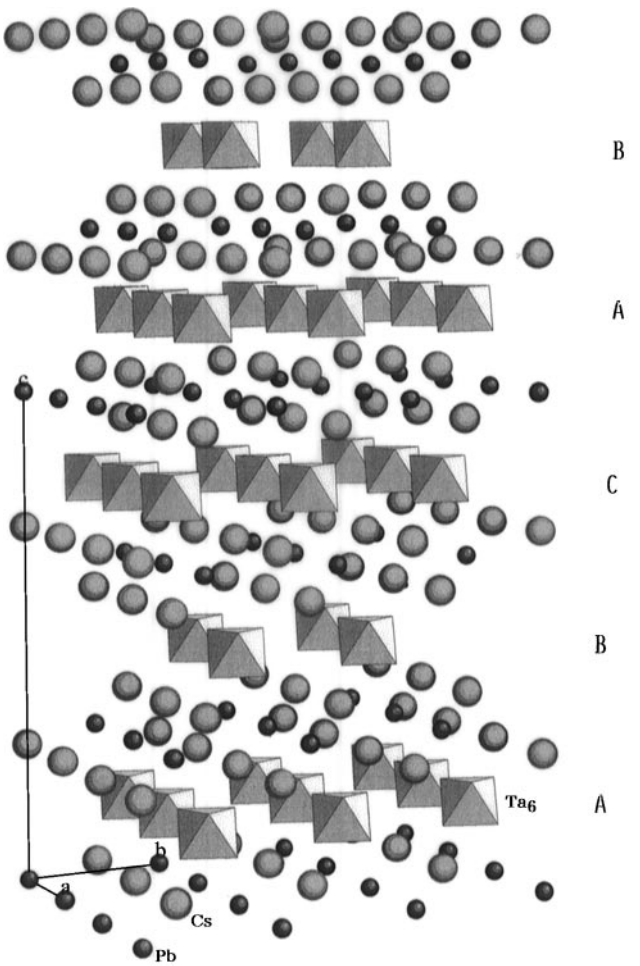

FIG. 3. Perspective view of the stacking of the Ta_6 clusters, Pb^{2+} and Cs^+, in the $Cs_2PbTa_6Cl_{18}$ hexagonal unit cell.

TABLE 8
Interatomic Distances (Å) and Angles (°) for $CsPbTa_6Cl_{18}$

	Ta_6 cluster		
Ta–Ta	2.9231(5)	Ta–Ta–Ta	59.96(1)
Ta–Ta	2.9272(6)	Ta–Ta–Ta	60.02(1)
	$(Ta_6Cl_{12})Cl_6$ unit		
Ta–Cl1	2.574(2)	Cl3–Ta–Cl1	82.22(7)
Ta–Cl2	2.438(2)	Cl2–Ta–Cl1	81.23(7)
Ta–Cl2	2.440(2)	Cl2–Ta–Cl1	82.86(8)
Ta–Cl3	2.435(2)	Cl3–Ta–Cl1	81.11(7)
Ta–Cl3	2.445(2)		
C12–C13	3.415(3)	Cl3–Cl2–Cl2	90.01(8)
C12–C13	3.411(3)	Cl3–Cl2–Cl2	59.96(2)
C12–C12	3.416(4)	Cl2–Cl3–Cl3	89.96(7)
C13–C13	3.418(2)	Cl2–Cl3–Cl3	60.07(7)
	Lead environment		
Pb–Cl1	2.902(2)	Cl1–Pb–Cl1	91.74(6)
	Cesium environment		
Cs–Cl1	3.616(2)		
Cs–Cl3	3.925(2)		
	Shortest other distances		
Pb–Cs	5.350(1)		
Pb–Pb	9.267(1)		
Cs–Cs	9.267(1)		
Ta–Pb	4.952(3)		
Ta–Cs	5.180(1)		

huge thermal factor is always observed in this structure type, even in an isotypic Zr_6 compound like $CsLaZr_6Cl_{18}$ (Fe) (12).

2. Comparison between the Distances within Ta_6Cl_{18} Units in the Two Compounds in Relation to Their Electronic Properties

The Ta–Ta intracluster distance is smaller in $Cs_2PbTa_6Cl_{18}$ (2.888 Å) than in $CsPbTa_6Cl_{18}$ (2.925 Å) relative to their VEC: 16 and 15, respectively. Indeed, in the latter case, the removal of one electron from the a_{2u} HOMO level (fully occupied with two electrons for VEC = 16), which exhibits a Ta–Ta bonding character with a Ta–Cl^i antibonding contribution (see Fig. 7), weakens the Ta–Ta bond which becomes longer. The short bond length found in $Cs_2PbTa_6Cl_{18}$ is in good agreement with the Ta–Ta distance (2.874 Å) in $CsErTa_6Cl_{18}$ with a VEC of 16 (see Table 9). Correlatively the Ta–Cl^i bonds become stronger as the VEC changes from 16 to 15. This trend can be seen in Ta–Cl^i distances found in both compounds.

It can be pointed out that Ta–Ta intracluster distances obtained for these two compounds are significantly shorter than the Nb–Nb distances usually encountered in Nb_6 cluster compounds with the same VEC in similar chloride series (Nb–Nb: 2.96 Å for VEC = 15 and 2.92 Å for VEC = 16). According to our previous theoretical studies (5), this feature can be related to relativistic effects on the *Me–Me* distances when going from third-row transition-metal elements to their second-row counterparts. In addition, the total width of the metallic *d* band has been found to be larger for tantalum than for niobium, reflecting that Ta–Ta interactions are stronger than Nb–Nb interactions.

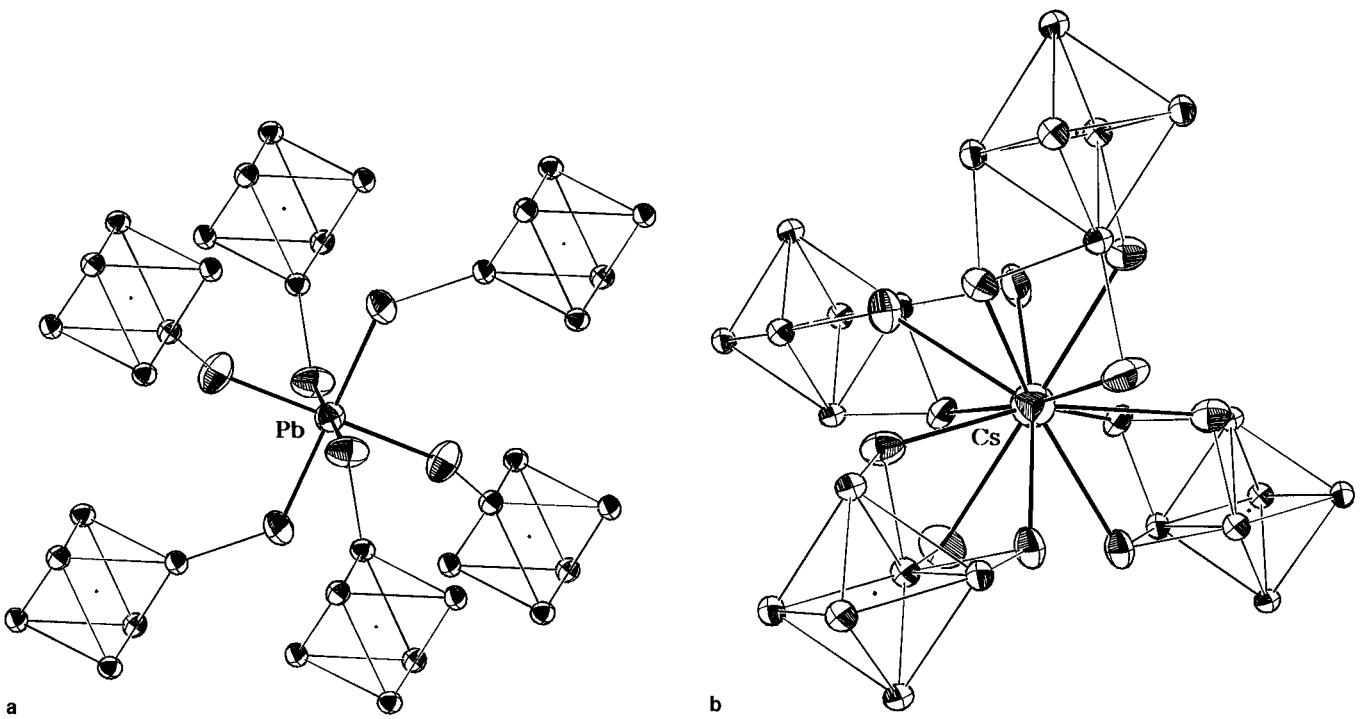

FIG. 4. Pb^{2+} (a) and Cs^+ (b) environments in the $Cs_2PbTa_6Cl_{18}$ structure. Only the Cl atoms involved in the Pb^{2+} and Cs^+ coordination spheres are shown.

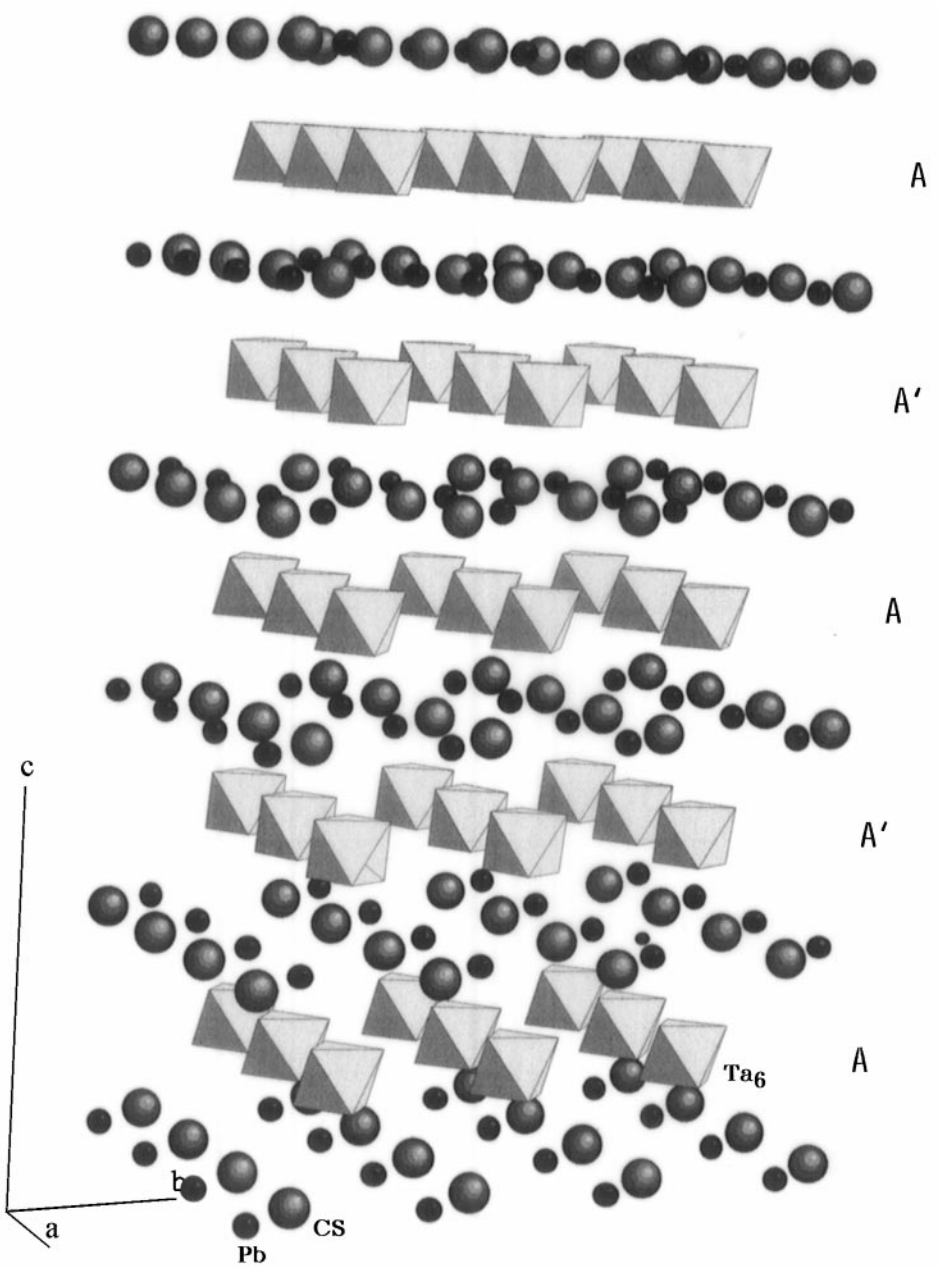

FIG. 5. Perspective view of the stacking of the Ta_6 clusters, Pb^{2+} and Cs^+, in the $CsPbTa_6Cl_{18}$ structure.

The evolution of the Ta–Cl^a distance is only due to Cl^a/Cl^i interaction or to the charge of the cation that is bonded to Cl^a, because the a_{2u} HOMO level has no Ta–Cl^a contribution (5). Indeed, in the two compounds presented here, the Ta–Cl^a distances are not very different, since in the two cases the apical chlorine is bounded to the same divalent cation. By comparison, the corresponding distance is longer in $CsErTa_6Cl_{18}$, the Cl^a ligand being more attracted by the trivalent erbium. A similar feature was observed in the Nb_6 bromide chemistry when comparing $CsErNb_6Br_{18}$ and $Cs_2EuNb_6Br_{18}$ with the same VEC of 16, in which Nb–Br^a was 2.885 and 2.804 Å, respectively (11). In the latter case, the shortening of the Nb–Br^a distances influences slightly the Nb–Nb intracluster distances by steric effects. Such a slight evolution of the Ta–Ta distances is similarly observed when comparing $Cs_2PbTa_6Cl_{18}$ and $CsErTa_6Cl_{18}$ (see Table 9).

IV. DISCUSSION

In the Me_6X_{18} unit-based halides obtained by solid-state routes, many compounds exhibit a VEC of 16, which

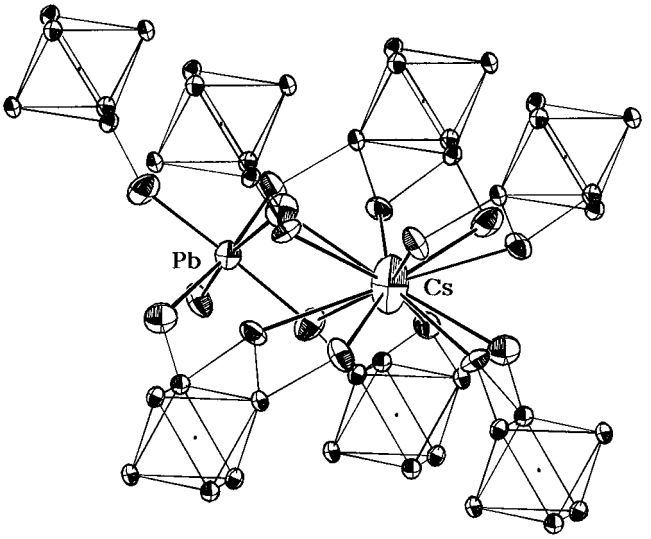

FIG. 6. Pb^{2+} and Cs^{+} environments in the $CsPbTa_6Cl_{18}$ structure. Only the Cl atoms involved in the Pb^{2+} and Cs^{+} coordination spheres are shown.

corresponds to the most stable oxidation state for the cluster. VEC = 15 has been obtained in a few examples: for the binary halides, Nb_6F_{15} (13) and Ta_6X_{15} (X = Cl, Br, I) (6), and for the ternary compounds, $REMe_6X_{18}$ in the Nb/Cl, Ta/Cl, and Ta/Br systems but not in the Nb/Br system (1). Me_6X_{18} unit-based halides with VEC = 14 have only been obtained by solution chemistry with large-sized and small-charged organic countercations which do not perturb too much the Me–X^a bonds (5). The $CsM'Ta_6Cl_{18}$ compounds presented in this paper constitute the first examples of quaternary halides with VEC = 15.

These observations concerning the VEC values obtained in the various Nb/Cl, Nb/Br, Ta/Cl, and Ta/Br systems are consistent with the DFT molecular orbital diagrams presented in Fig. 7 for different Me_6X_{18} systems. This calculation has been performed from average experimental data and is fully detailed in a separate publication (5). One can see that ΔE_2 is always larger than ΔE_1 which explains the greater stability of VEC = 16 compounds in all systems, which also corresponds to the total filling of MOs with Me–Me bonding character; the energy of the a_{2u} level is constant overall. On the other hand, ΔE_1 hardly varies with the nature of the metal, but is significantly influenced by the nature of the ligands. Indeed, Me–X^a antibonding contribution is observed for the lowest Me–Me bonding-occupied MOs. Consequently, increasing this antibonding character, for instance, when the electronegativity of the apical ligand becomes closer to that of the metal, leads to destabilization of these MOs, which induces a decrease in ΔE_1. This is the case for bromine compared with chlorine, and as a consequence, it is easier to obtain chlorides with $15e^-/Nb_6$ than bromides. ΔE_2 strongly varies with the nature of the metal: Ta–Ta interactions are stronger than Nb–Nb interactions

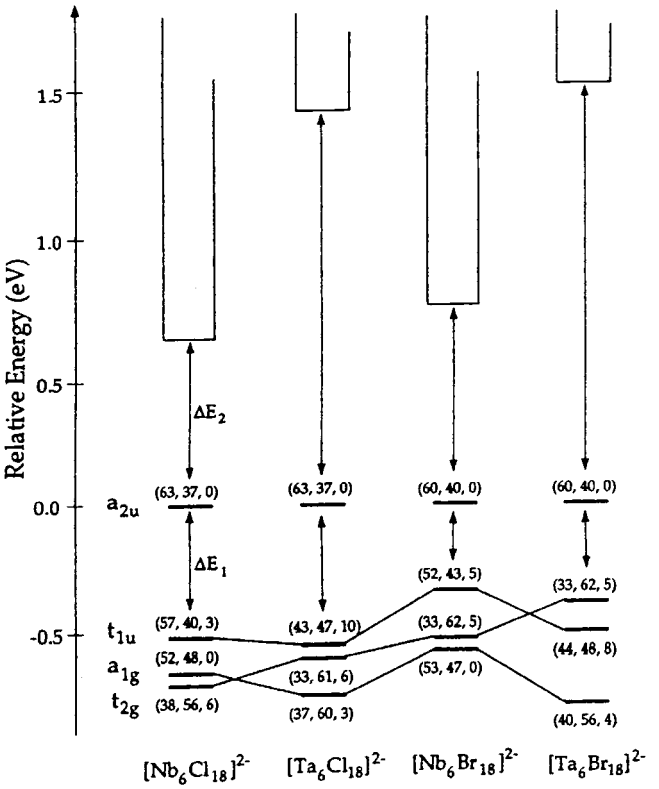

FIG. 7. SR-DFT energy level diagrams for 14-electron $[(Me_6X^i_{12})X^a_6]^{2-}$ models taken from (5); numbers in parentheses indicate the percentages of Me, X^i, and X^a, respectively.

which gives a stronger Me–Me antibonding character for the lowest vacant MOs positioned above the a_{2u} MO; this produces a larger width for ΔE_2 in the case of tantalum. All these considerations could explain why Nb_6Br_{18} unit-based compounds are observed with VEC = 16 but not VEC = 15, while a VEC of 15 can be more easily obtained in the Ta/Cl system which exhibits a larger ΔE_1 gap and stronger Ta–Ta interactions than Nb–Nb interactions.

In conclusion, the possibility of obtaining $CsEuTa_6Cl_{18}$ with the divalent europium and a VEC of 15, instead of trivalent europium with a VEC of 16 as always previously encountered for all other compounds in the P-31c series,

TABLE 9
Average Distances (Å) within Me_6X_{18} Units in Selected Ta_6 and Nb_6 Compounds

	Ref.	Space group	VEC	Me–Me	Me–X^i	Me–X^a
$CsPbTa_6Cl_{18}$	This work	P-31c	15	2.925(1)	2.439(2)	2.574(2)
$Cs_2PbTa_6Cl_{18}$	This work	R-3	16	2.888(1)	2.462(2)	2.595(2)
$CsErTa_6Cl_{18}$	(5)	P-31c	16	2.874(1)	2.463(2)	2.691(2)
$Cs_2EuNb_6Br_{18}$	(11)	R-3	16	2.970(1)	2.595(1)	2.804(1)
$CsErNb_6Br_{18}$	(11)	P-31c	16	2.954(1)	2.587(1)	2.885(2)

confirms the discussion developed above. Thus, we can assume that the easier way to obtain clusters with VEC = 15 is to synthesize compounds in the Ta_6 chloride chemistry. These VEC = 15 compounds are of special interest because they exhibit paramagnetic behavior due to the presence of one unpaired electron on the a_{2u} HOMO level (2, 6, 14, 15). Unfortunately, the limited purity of the $CsM'Ta_6Cl_{18}$ microcrystalline powders and the great difficulty encountered in obtaining single crystals of significant size in the Ta_6 halide chemistry, have not allowed us to perform rigorous magnetic measurements of these halides, until now.

ACKNOWLEDGMENT

This work has been supported in part by Fondation Langlois which is warmly acknowledged.

REFERENCES

1. C. Perrin, S. Cordier, S. Ihmaïne, and M. Sergent, *J. Alloys Compds.* **229,** 123 (1995).
2. S. Ihmaïne, C. Perrin, O. Peña, and M. Sergent, *J. Less-Common Met.* **137,** 323 (1988).
3. S. Ihmaïne, C. Perrin, and M. Sergent, *Acta Crystallogr. Sect. C* **45,** 705 (1989).
4. J. Sitar, A. Lachgar, H. Womelsdorf, and H.-J. Meyer, *J. Solid State Chem.* **122,** 428 (1996).
5. F. Ogliaro, S. Cordier, J.-F. Halet, C. Perrin, J.-Y. Saillard, and M. Sergent, *Inorg. Chem.* **37,** 6199 (1998).
6. D. Bauer and H. G. von Schnering, *Z. Anorg. Allgem. Chem.* **361,** 259 (1968).
7. N. Walker and D. Stuart, *Acta Crystallogr. A* **39,** 158 (1983).
8. G. Stout and L. H. Jensen, "X-ray Structure Determination." MacMillan, London, 1968.
9. "International Tables for X-ray Crystallography," Tome IV, Kynoch Press, Birmingham (distributor: D. Reidel, Dordrecht), 1975.
10. C. K. Fair, "MOLEN: An Interactive Intelligent System for Crystal Structure Analysis." Enraf Nonius, Delft, 1990.
11. S. Cordier, C. Perrin, and M. Sergent, *Z. Anorg. Allgem. Chem.* **619,** 621 (1993).
12. J. Zhang and J. D. Corbett, *Inorg. Chem.* **32,** 1566 (1993).
13. D. Bauer, H. G. von Schnering, and H. Schäfer, *J. Less-Common Met.* **8,** 388 (1965).
14. J. G. Converse and R. E. McCarley, *Inorg. Chem.* **9,** 1361 (1970).
15. O. Peña, S. Ihmaïne, C. Perrin, and M. Sergent, *Solid State Commun.* **74,** 285 (1990).